General continuum theory for multiion channel

I. Theory

David G. Levitt
Department of Physiology, University of Minnesota, Minneapolis, Minnesota 55455 USA

ABSTRACT It is assumed that the channel is completely characterized by three factors: (*a*) its geometric shape, (*b*) the potential energy interaction between an ion and the channel wall, and (*c*) the potential energy interaction between two ions at arbitrary positions in the channel. The total potential energy of an ion in a multiion channel can be described by a summation over factors *b* and *c*. The ion–water interaction is described by a continuum diffusion coefficient which is determined by the channel geometry (*c*). Given this physical description, a theory is described that predicts the flux of all the ion species that are present, with no additional assumptions about, e.g., the maximum number of ions allowed in the channel, location of binding sites or shape of energy barriers. The solution is based on a combination of the Nernst–Planck and Poisson equation. The Poisson potential is corrected for the ion's self potential. A hard sphere ion–ion interaction is included that prevents ions from piling up on top of each other in regions where the channel wall has a high charge density. An exact analytical solution is derived for the region in the bulk solution far from the channel mouth and this solution is used as a boundary condition for the numerical solution. The numerical solution is obtained by an interactive procedure that is surprisingly efficient. Application of the theory to the acetylcholine receptor channel is described in the companion paper (Levitt, D. G. 1990. *Biophys. J.* 59:278–288).

INTRODUCTION

Detailed information about the molecular structure of biological ion channels is now becoming available. In particular, site directed mutagenesis of the acetylcholine receptor channel (ACH) has identified a set of α-helices that probably form the channel wall (Imoto et al., 1988). Experimental modification of the charges at the ends of these helices produced the expected qualitative changes in conductance. From the synthesis of these results and those of a number of other studies, a low resolution picture of the conduction pathway of the ACH channel has now emerged (Dani, 1989).

Given this unprecedented structural information, an obvious next step is to try to predict the resulting ion conductance. Ideally, one would like to determine this ion flux just on the basis of a physical description of the channel, with no additional assumptions about, for example, the location of binding sites, shape of energy barriers or maximum number of ions allowed in the channel. It will be assumed here that a physical description of the channel consists of three elements: (*a*) the channel geometry, (*b*) the interaction potential between the channel wall and an ion at an arbitrary position in the channel, and (*c*) the interaction potential between any two ions present at arbitrary positions. These three factors provide a complete description of the channel kinetics. The multiion interaction can be obtained by a summation over the individual ion–ion interactions. The interaction between the water and ion is modeled in terms of a continuum diffusion (frictional) coefficient which is uniquely determined by the channel geometry.

The purpose of this paper is, given these three physical functions, to solve for the flux of the different ions. No assumption will be made about, for example, the origin of the ion–ion or ion–wall forces. They may be from long range fixed charges, shorter range dipoles, or very short range steric forces. There is, however, one fundamental limitation that is imposed on the forces. It is assumed that the potential functions are constant over the cross-section of the pore. This is only approximately correct, and the shorter the range of the force, the less correct this assumption will be.

If ion–ion interaction can be neglected, then the Nernst–Planck equation provides an exact general solution for the above physical model (Levitt, 1986):

$$J_i = -A_i D_i \left[\frac{dC_i}{dX} + \frac{z_i e}{kT} C_i \frac{dU_i}{dX}\right], \tag{1}$$

where J_i is the steady-state flux of ion species i, D_i is the diffusion coefficient (and is a function of the spatial position), C_i is the (number) ion concentration, the potential energy U_i is the explicitly modeled ion–wall interaction, z_i is the ion's valence, e is the electron charge, k is Boltzmann's constant, and R is the gas

---

Address correspondence to David Levitt, Department of Physiology, 6-255 Millard Hall, University of Minnesota, Minneapolis, MN 55455.

Biophys. J. © Biophysical Society
Volume 59 February 1991 271–277
0006-3495/91/02/271/07 $2.00

constant. It has been assumed in Eq. 1 that C and U are constant over the cross-sectional area of the channel and $A_i(x)$ is the area available to ion species i. Eq. 1 has a simple analytical solution in which the flux can be expressed in terms of the function U_i (Levitt, 1986).

If ion–ion interaction cannot be neglected, then U_i becomes a function of the position of the other ions, which are all correlated with each other, and Eq. 1 cannot be used because it no longer provides a complete description of the system. The solution to Eq. 1 is linear in the concentration (C_i). Any deviation from this linearity is evidence of ion–ion interaction. Because the conductance of most biological ion channels saturates as the concentration is raised (usually in the physiological concentration range), Eq. 1 is not applicable to these channels. The ability to describe this saturation is an essential requirement of any model. In all previous models of ion channels, this saturability has been introduced in an *ad hoc* way. For example, in reaction-rate models, the number of ion sites and the maximum number of ions in the channel are predetermined and this naturally leads to a maximum flux rate (Levitt, 1986). Saturation can also be demonstrated in continuum models in which the maximum number of ions (either one [Levitt, 1986] or two [Levitt, 1987]) allowed in some limited region of the channel is added as an auxiliary condition. In contrast, in the ideal model, saturation should follow directly from just a physical description of the channel with no added conditions.

One way to generalize Eq. 1 is to take explicit account of the position of all the ions in the channel. In this case, C is replaced by a function that describes the probability of finding the ions at each position and Eq. 1 is replaced by a partial differential equation. This procedure has been carried out for the case where there are, at most, two ions in the channel (Levitt, 1987). Although it can be extended to higher numbers of ions, the high order increase in computational requirements makes solutions beyond three ions impractical. A more generally applicable approach is that of Brownian dynamics where the time evolution is directly simulated on the computer with the local ion–water interaction modeled by a simple frictional term (Cooper et al., 1985). This approach has the major advantage that the computational requirements have only a weak dependence on the number of ions. Such simulations are very computationally intensive and have only been carried out for small model channels with, at most, two interacting ions. Application of Brownian dynamics to large channels, e.g., the ACH channel, is probably possible now on large computers. A factor that limits the accuracy of these simulations is the way the bulk solution at the channel mouth is modeled. To limit the size of the system, at some point the bulk solution must be replaced by a boundary condition whose influence on the solution is uncertain.

The purpose of this paper is to describe a solution that provides a good approximation to the above problem and yet is not computationally demanding. The solution is based on a combination of the Nernst–Planck and Poisson equations (deLevie et al., 1972; Levitt, 1985). It has a number of novel features: (*a*) a hard sphere ion–ion repulsive potential is included. This is an essential feature because it prevents ions from piling up on top of each other in regions of the channel that have a large channel wall charge. (*b*) The ion's self potential is subtracted from the total potential acting on the ion in the solution of the Poisson equation. (*c*) An exact analytical solution is obtained for the bulk solution far from the channel mouth and this is used to provide accurate boundary conditions for the region that must be solved numerically. These three features have not been used in any previous model. They can lead to large effects on the conductance and should significantly increase the accuracy of the solution. (*d*) The entire solution is for the nonequilibrium regime. It is not necessary to assume, for example, that the ions are at equilibrium in the solution of the Poisson equation. (*e*) An arbitrary number of different ions with arbitrary size, valence and diffusion coefficient can be included without significantly increasing the computation time. (*f*) A simple iterative solution is used. A typical solution requires ~1 min on a 25 mHz IBM type microcomputer. (The code is written in Pascal and is available upon request.) The general solution will be described below and the application to the ACH channel will be described in the following paper (Levitt, 1990).

GENERAL SOLUTION

Flux equation

A schematic diagram of a general channel model is shown in Fig. 1. The fundamental assumption is that the flux can be described by Eq. 1 with U modified to include the interactions with all the other ions that are present. The equation will be rewritten in terms of the following dimensionless variables:

$$j_i = -a_i d_i \left[\frac{dc_i}{dx} + z_i c_i \gamma \frac{du_i}{dx}\right]$$

$$j_i = \frac{R^2 J_i}{D_i^\circ} \quad a = \frac{A}{2\pi R^2} \quad c = 2\pi R^3 C \quad x = \frac{X}{R} \quad d_i = \frac{D_i}{D_i^\circ}$$

$$u = \left(\frac{\epsilon_w R}{e}\right) U \quad \frac{eU}{kT} = \gamma u \quad \gamma = \frac{e^2}{kT\epsilon_w R}, \tag{2}$$

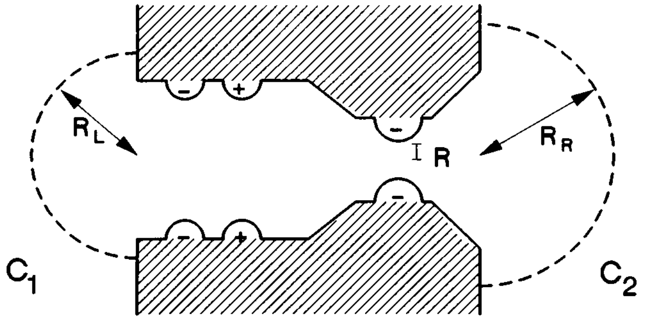

FIGURE 1 Schematic model of channel. The channel wall has an arbitrary geometric shape and distribution of surface charges. The constant R is the radius at some specific location and is used to normalize the parameters, and R_L and R_R are the radial distances from the channel mouth where the analytical boundary condition is used.

where R is the pore radius at some characteristic position (e.g., the ion binding site, Fig. 1), D_i^0 is the bulk diffusion coefficient of the ith ion, and ϵ_w is the dielectric constant of water. The dimensionless constant γ appears frequently in the following equations. When R is in angstroms, its numerical value is $6.96/R$.

Potential functions

The potential u in Eq. 2 will be written as the sum of four terms:

$$u_i = w_i + (\text{hard sphere potential})$$
$$w_i = v + \phi_w^i + \phi_d, \tag{3}$$

where v is the applied voltage, ϕ_w is the potential from the channel wall, and ϕ_d is the diffuse electrostatic potential from all the other ions (and does not include the ion's self potential) and is obtained from a solution of Poisson's equation (see below). The ion–ion interaction term includes the "image" force of all the ions. The wall potential (ϕ_w) includes the electrostatic potential from the fixed pore changes, the Born image potential, and, possibly, other more short range forces, and is assumed to be a given, known function.

In addition to these long-range electrostatic potentials, a short-range hard sphere repulsive potential must be included. For example, if the "binding site" has a net charge of -2, the long-range potential will attract two monovalent cations to positions in which their hard sphere radii overlap. To prevent this the hard sphere term in Eq. 3 is introduced, defined as follows. Assume that the equilibrium concentration is described by an equation of the form:

$$\frac{C_i(x)}{P_0(x)} = e^{-z_i\gamma w_i}, \tag{4}$$

where $P_0(x)$ is the average probability that there is no ion in the excluded volume centered about x (determined by integrating $c_i(x)$ over this volume and summing over i). As the concentration rises, P_0 approaches zero, guaranteeing that there is at most one ion in any excluded volume. This is analogous to the excluded volume term in Van der Waals equation. Assuming that this relation is true for the general, nonequilibrium case, the total potential u will be defined by:

$$e^{-z_i\gamma u_i} = P_0 e^{-z_i\gamma w_i}. \tag{5}$$

In the simple case of the interaction between two hard spheres, the radius of the excluded volume is equal to the distance between the ion centers which is equal to the sum of the radii of the two ions. Thus, the excluded volume of one ion depends on the radius of the ion it is interacting with. Because in the approximation used here, all the ions acting on the central ion are replaced by a diffuse charge, it is not possible to allow the excluded volume to depend on the ion type and it is assumed that this volume is the same for all ions.

General expression for the concentration

Eq. 2 has exactly the same form as the simple Nernst–Planck equation (Eq. 1) and it can be solved the same way. Eq. 2 can be rewritten in the form:

$$j_i \frac{e^{z_i\gamma u_i}}{a_i d_i} = -\frac{d\bar{c}_i}{dx} \quad \bar{c}_i = c_i e^{z_i\gamma u_i}. \tag{6}$$

Integrating Eq. 6 from the left bulk solution ($-\infty$) to the right bulk solution ($+\infty$):

$$j_i = (\bar{c}_{i1} - \bar{c}_{i2})/h_i(\infty) \quad h_i(x) = \int_{-\infty}^{x} \frac{e^{z_i\gamma u_i}}{a_i d_i}. \tag{7}$$

In the bulk solution, far from the channel, ϕ_w and ϕ_d (defined relative to the bulk solution value) are zero, and P_0 is assumed to be one (so that the concentration approaches the bulk value):

$$\bar{c}_{i1} = c_{i1} e^{z_i\gamma v_1} \quad \bar{c}_{i2} = c_{i2} e^{z_i\gamma v_2}, \tag{8}$$

where c_{i1}, v_1, c_{i2}, and v_2 are the concentration and voltage in the left and right bulk solution. Integrating Eq. 6 from $-\infty$ to x and solving for c:

$$c_i(x) = P_0 e^{-z_i\gamma w_i}[\bar{c}_{i1} - j_i h_i(x)]. \tag{9}$$

Special case: one-ion channel

Before describing the general solution, consider the following special case. Assume that (a) there is some region ($0 < x < L$) of the channel (referred to as the "one-ion region") that can be occupied by at most one ion and that (*b*) outside this region, the ions are at equilibrium with the bulk solution on the same side. Assumption *b* is equivalent to the assumption that the factor $a_i d_i$ is infinite external to the one-ion region. Thus, this one-ion region becomes rate limiting and, in this region, $P_o(x)$ is a constant (P_o). Also, the contribution to ϕ_d from the one-ion region is zero because, by definition, no other ions are present and it will be assumed that the contribution from outside this region is negligible. The flux (Eq. 7) then reduces to:

$$j_i = \frac{P_o[\bar{c}_{i1} - \bar{c}_{i2}]}{g_i(L)} \quad g_i(x) = \int_0^x \frac{e^{z_i\gamma(v+\phi_w^i)}}{d_i a_i}. \tag{10}$$

The value of P_o is obtained from:

$$P_1 = 1 - P_o = \sum_i \int_0^L a_i c_i dx = P_o B$$

$$B = \sum_i \int_0^L a_i e^{-z_i(\phi_w+v)}\left[\bar{c}_{1i} - (\bar{c}_{1i} - \bar{c}_{2i})\frac{g(x)}{g(L)}\right] dx, \tag{11}$$

where the expression for $c(x)$ (Eq. 9) has been used in Eq. 11. Finally, solving Eq. 11 for P_o:

$$P_o = 1/(1 + B). \tag{12}$$

Eqs. 10–12 provide a simple analytical solution for the flux. It is identical to that of the "one-ion channel" result derived previously (Levitt, 1986). The two above assumptions which lead to this result differ from those used in the earlier derivation and appear to be more physically realistic. A more important advantage of this derivation is that it clearly indicates how these assumptions can be relaxed and the solution extended to the general multi-ion channel by replacing the constant P_o by the variable function $P_o(x)$.

General expression for P_o

For the general case, P_o is defined by:

$$P_1(x) = 1 - P_o(x) = \sum_i \int_{V_h(x)} c_i(\alpha)d\alpha, \tag{13}$$

where c_i (normalized as described in Eq. 2) is given by Eq. 9 and the integral is over the excluded volume (V_h) of the ion and the summation is over all the ion species (Na^+, Cl^-, Mg^{++}, etc.). For example, if two ions can touch each other, then the excluded volume is equal to a sphere with a radius equal to the sum of the radii of the two ions. The solution will be obtained iteratively, substituting the concentration from the previous iteration into Eq. 13 to determine the value of $P_o(x)$ for the next iteration.

Diffuse potential (ϕ_d)

In the general model, the interaction between ions arises from both the P_o term and the potential ϕ_d, the electrostatic interaction with all the other ions in the channel. Poisson's equation in the channel can be approximated by (Levitt, 1985):

$$(a_e\phi')' = -2\sum_i z_i a_i c_i. \tag{14}$$

The potential $\phi(x)$ that is obtained from a solution of Eq. 14 (see Appendix) is the electrostatic potential at x from all the mobile ions in the channel. It is not equal to $\phi_d(x)$ because $\phi(x)$ is the potential from all the ions, whereas $\phi_d(x)$ should not include the self potential from the ion at x. Thus, ϕ_d is defined by:

$$\phi_d(x) = \phi(x) - \phi_s(x)$$

$$\phi_s(x) = \sum_i \int_{V_h(x)} F(\alpha, x) z_i c_i(\alpha) d\alpha, \tag{15}$$

where $\phi_s(x)$ is the self potential and is equal to the potential at x from all the ions within the excluded volume at x ($F[\alpha, x]$ is the potential at x for a charge at α). The solution is obtained iteratively with the concentration (c_i) from the previous iteration used to find ϕ_s for the next iteration.

The derivation of Eq. 14 is based on the assumption that the perpendicular component of the electric (E) field in the aqueous solution at the pore wall is negligible compared to the parallel component. This assumption, which has been discussed in detail previously (Levitt, 1985), should be a good approximation for most ion channels. It is assumed that the E field is constant over the electrostatic surface area (a_e in Eq. 14). Decreasing a_e increases the strength of all the electrostatic fields in the channel, and a_e can be regarded as an adjustable parameter, characterizing the strength of these fields. It should be larger than a_i (the physical area available to the ith ion), especially if the lining of the channel has a high dielectric constant.

Boundary conditions

In the bulk solution, far from the channel mouth, the potential u is small and an analytical solution to Eq. 14 can be found (see Appendix). This analytical solution can then be used to provide boundary conditions for the left (L) and right (R) sides of the numerical region:

$$\text{at}\ x = r_L\text{:}\ \frac{d\phi}{dx} = \left(\kappa_1 + \frac{1}{r_L}\right)\phi + \kappa_1(\phi_w + v - v_1) + \frac{2I}{\kappa_1 r_L}$$

$$\text{at}\ x = r_R\text{:}\ \frac{d\phi}{dx} = -\left(\kappa_2 + \frac{1}{r_R}\right)\phi - \kappa_2(\phi_w + v - v_2) + \frac{2I}{\kappa_2 r_R}$$

$$\kappa_1^2 = 2\gamma \sum_i z_i^2 c_{i1} \quad \kappa_2^2 = 2\gamma \sum_i z_i^2 c_{i2} \quad I = \sum_i z_i j_i \tag{16}$$

where κ_1 and κ_2 are the Debye constant for the left and right bulk solutions, r_L and r_R are the radial distance of the boundary position from the pore mouth on the left and right side (see Fig. 1), and I is the total current.

General solution procedure

This completes the description of the general multiion channel. The channel is characterized by a_i (the cross-sectional area available to the ion) and the position and value of the fixed channel wall charges from which the electrostatic contributions to ϕ_w (including the Born image potential) and v can be determined. If an additional, nonelectrostatic wall force is postulated, then it must be explicitly described. Although the value of the diffusion coefficient (D_i) can be estimated from continuum theory for the regions of the pore that have a large radius (Levitt, 1975), it is unknown in narrow regions and may be regarded as an adjustable parameter.

The solution is obtained iteratively. The value of c_i from the previous iteration (or a guess for the first iteration) is used to find ϕ (finite difference solution to Eq. 14 with Eq. 16 as the boundary condition), ϕ_d (Eq. 15), and P_o (Eq. 13). Then, from these values of ϕ_d and P_o, a new value of u_i is found (Eqs. 3 and 5) from which the flux j_i (Eq. 7) is determined. Finally, a new estimate of c_i is determined from Eq. 9 and the procedure is started again. The iteration is repeated until the value of j_i converges to a limiting value.

The details of the implementation of the solution are described in the Appendix and the accompanying paper illustrates the application of this procedure to a channel with a structure similar to that predicted for the ACH channel. The major limitation of the method is that, if the local channel wall fixed charge density is too large, the solution either does not converge or converges very slowly. Several general modifications of the procedure to improve the rate of convergence are described in the Appendix. With these modifications, the rate of convergence is surprisingly fast and stable over a wide range of model conditions (Levitt, 1990). The addition of the hard sphere repulsive term significantly improves the stability of the solution.

DISCUSSION

High concentration limit

As mentioned in the Introduction, saturation of the current with increasing concentration is a characteristic experimental feature of most biological ion channels. (In the gramicidin channel, the flux actually tends to decrease at high concentrations. This probably results from the presence of multiple "binding sites" and the dominant single file effects that are present in gramicidin and is not likely to be representative of biological channels.) This is a somewhat paradoxical observation because, as is shown by the following qualitative argument, one would predict theoretically that most channels would not saturate. Consider the channel model shown in Fig. 1. For the case where the binding site region has a fixed charge greater than one there will be a net attractive potential to this site even when it is already occupied by a monovalent ion. One would predict that, as the concentration is raised, there should be an increasing probability of finding this second ion near the first ion and the repulsive ion–ion interaction should lead to an increased conductance, preventing saturation.

The model described in this paper provides a more quantitative basis for predicting the channel properties that are necessary for saturation. At high concentrations, the probability that the binding site region is occupied by an ion will approach one and $P_o \approx 0$ (for a specific example, see Levitt, 1990; Fig. 8). Because of the hard sphere repulsive potential, P_o is approximately constant and close to zero in the excluded region around the binding site. Approximating $P_o(x)$ by a constant in this region, the general expression for the flux (Eq. 7) can be written in the form:

$$j_i \approx \frac{(\bar{c}_{i1} - \bar{c}_{i2})}{h_w + g_o/P_o} \quad g_o = \int_{V_{h(o)}} \frac{e^{z_i \gamma w_i}}{a_i d_i} d\alpha, \tag{17}$$

where the integral h has been divided into a term arising from the integral over the excluded region around the binding site (g_o/P_o) and the rest of the integral (h_w). As the concentration is raised, P_o will approach zero and the g_o/P_o term will dominate the denominator of Eq. 17. This means that the ion binding site region becomes the rate limiting step in ion transport and the rest of the channel is approximately in equilibrium with the bulk solution.

In this limit ($P_o \rightarrow 0$), the conductance becomes similar to the one-ion channel described in Eqs. 10–12 (assuming $c_1 = c_2$):

$$
\begin{aligned}
j_i^{\max} &= (e^{z_i\gamma v_1} - e^{z_i\gamma v_2})/(g_o b) \\
b &= \sum_i \int_{-x_h}^{x_h} a_i e^{-z_i w_i}[e^{z_i\gamma v_1} - (e^{z_i\gamma v_1} - e^{z_i\gamma v_2})g(x)/g_o]\,dx \\
g(x) &= \int_{-x_h}^{x} d\alpha e^{z_i\gamma w_i}/(d_i a_i),
\end{aligned}
\tag{18}
$$

where the excluded region about the binding site extends from $-x_h$ to $+x_h$.

Although the solution concentrations (c_1, c_2) have canceled out of Eq. 18, the conductance should still be influenced by the concentration because increasing the concentration will increase the number of ions outside the excluded region and these ions, through ϕ_d (which is part of w), will result in an increase in conductance. This argument suggests that a requirement for saturation is that the one ion region is large enough that the ions external to it have only a minor influence on the ion at the "binding site." Alternatively, if the attractive potential at the binding site has a short range (as opposed to the long range fixed charge potential) then ϕ_d should be small outside this region, and saturation should occur.

Validity of model

The obvious question to be asked about this model is "how good is it?" Each time the ion passes through the channel it interacts with only a finite set of ions. In an exact solution, one would average over a long time in which many ions passed through the channel, each interacting with different arrangements and numbers of other ions. The major assumption of this model is that this time average interaction with a small number of ions can be replaced by an interaction with a continuum of ions whose distribution is equal to the spatial average concentration (subtracting the self contribution). This is analogous to the self-consistent field approach. Although this assumption should be qualitatively valid, the only way to evaluate its quantitative accuracy is to compare it with a more exact solution, such as a Brownian dynamic simulation.

One would expect that this model would be quite accurate in describing the maximum flux at high concentrations (Eq. 18) because, in this limit the kinetics reduce to that of a one-ion channel (the other ions are approximately at equilibrium), a case this model is ideally suited for. This limit may also represent the most important practical use of this model. Because most biological channels are close to saturation in the physiological concentration range, it should be relatively easy to investigate the properties of the current at high concentrations (voltage dependence, asymmetry, divalent–monovalent interaction, etc.) and use Eq. 18 to relate these properties to the structure of the binding site region.

APPENDIX

I. Analytical solution to Eq. 14 and derivation of boundary conditions (Eq. 16)

The solution is obtained in the bulk solution far from the channel where the ion–wall interaction potential is small. The solution will be described for the region at the left end of the channel (Fig. 1, $-\infty < r < -r_L$). It is assumed that in this region: (*a*) the electrostatic field and the ion flux is directed radially and that the electrostatic area (A_e) and the area available to the ion (A_i) are equal to $2\pi R^2$, where R is the radial distance from the channel mouth ($a_e = a_i = a = r^2$; $r = R/R_o$); (*b*) $P_o = 1$; (*c*) $\phi_s = 0$, so that $\phi_d = \phi$; (*d*) the Born potential is zero so that $w_i = w$; (*e*) $d_i = 1$. The right hand side of Eq. 14 can then be written as:

$$
\begin{aligned}
2a \sum_i z_i c_i &= 2a \sum_i z_i e^{-z_i\gamma w}[c_{i1} e^{z_i\gamma v_1} - j_i h_i] = F_1 + F_2 \\
F_1 &\approx 2a \sum_i z_i c_{i1}[1 - z_i\gamma(w - v_1)] = a\kappa_1^2(\phi_w + \phi) \\
F_2 &\approx -2a \sum_i z_i j_i e^{-z_i\gamma w} \int_{-\infty}^{r} \frac{e^{z_i\gamma w}}{\alpha^2}\,\mathrm{d}\alpha \approx 2rI,
\end{aligned}
\tag{1A}
$$

where I and κ_1 are defined in Eq. 16. In the F_1 expression in Eq. 1A, the exponential can be expanded because ϕ is small in this region. In F_2 the major contribution from the integral will come from the region near $\alpha = r$, and it is assumed in the second equality that, in this region, w is constant. This approximation introduces only a small error because, for large r, $F_2 \ll F_1$.

Poisson's equation for this region then reduces to:

$$(a\phi')' = r^2\kappa_1^2(w - v_1) - 2rI. \tag{2A}$$

Defining $y = w - v_1$, then in this region:

$$(a\phi_w')' = (av')' = 0 \Rightarrow (ay')' = (a\phi')', \tag{3A}$$

and Eq. 2A can be written as ($a = r^2$):

$$(r^2 y')' = k_1^2 r^2 y - 2rI. \tag{4A}$$

This has the solution:

$$y = \frac{B}{r} e^{\kappa_1 r} + \frac{2I}{\kappa_1^2 r}, \tag{5A}$$

where B is an arbitrary constant. Finally, substituting the definition of y, finding y' and using Eq. 3A, yields the boundary condition at $r = -r_L$ (Eq. 16). A similar relation can be derived for the right end ($r = r_R$, Eq. 16).

II. Detail of numerical solution

Although the procedures described below were specifically used to improve the solution for the channel resembling the ACH receptor (Levitt, 1990), they are of a quite general nature and should be useful for most channels.

A. Concentration expression

Eq. 9 was derived by integrating Eq. 6 for $-\infty$ to x. A similar expression can be obtained by integrating from x to $+\infty$:

$$c_i(x) = P_o e^{-z_i\gamma w_i}[\bar{c}_{i2} + j_i(h_i(\infty) - h_i(x))]. \tag{6A}$$

In the solution for the ACH channel, Eq. 9 was used when x was to the left of the binding site and Eq. 6A was used for x to the right of the binding site.

B. Numerical solution of Eq. 14

Eq. 14 is solved by a finite difference method at grid points x_j ($j = 0-n$) where the jth equation is:

$$A_j\phi_{j-1} + B_j\phi_j + C_j\phi_{j+1} = D_j$$

$$A_j = (a_e)_{j-1/2} \quad B_j = -(a_e)_{j-1/2} - (a_e)_{j+1/2} \quad C_j = (a_e)_{j+1/2}$$

$$D_j = -2\Delta^2 \sum_i z_i a_i P_o(\bar{c}_{i1} - j_i h_i)e^{-z_i\gamma w_i} \qquad \Delta = x_{j+1} - x_j, \tag{7A}$$

and the boundary conditions (Eq. 16) are used to eliminate the $j = -1$ and $j = n + 1$ terms. The rate of convergence of the solution is markedly improved if the following expansion is used. At the $k + 1$ iteration, the exponential in the D_j term can be written as:

$$\begin{aligned}\exp(-z_i\gamma w_i^{k+1}) &= \exp(-z_i\gamma(w_i^{k+1} - w_i^k) \exp(-z_i\gamma w_i^k)\\ &\approx \exp(-z_i\gamma w_i^k)[1 - z_i\gamma(\phi^{k+1} - \phi^k)].\end{aligned} \tag{8A}$$

Thus, D_j is equal to:

$$D_j^{k+1} \approx D_j^k(1 + z_i\gamma\phi^k) - D_j^k z_i\gamma\phi^{k+1}. \tag{9A}$$

Finally, the ϕ^{k+1} term in Eq. 9A is moved to the left side of Eq. 7A (the B_j term) and D_j is redefined as equal to the ϕ^k term in Eq. 9A.

C. Solution for self potential (ϕ_s)

In Eq. 9 for c, ϕ_s (Eq. 15) appears as a positive exponential. This makes the iteration unstable if ϕ_s is large because an increase in ϕ_s leads to an increase in c which leads to a further increase in ϕ_s. To avoid this, the binding site region of the channel where ϕ_s is large is treated in a special way. It is assumed that, in the calculation of ϕ (Eq. 14) that there are no other ions in some region (v_1) around the binding site region. Thus, in this region, the correction for ϕ_s is not needed. The diffuse potential contribution from this region (ϕ_1) is calculated separately:

$$\phi_1(x) = \sum_i \int_{v'_i} F(\alpha, x) z_i c_i(\alpha) d\alpha, \tag{10A}$$

where v'_1 is equal to v_1 minus any overlap with the ion's excluded volume at x (see Eq. 15 for a definition of F).

D. Solution for P_o

The definition of P_o in Eq. 13 ($P_o = 1 - P_1$) cannot be used because P_1 can be very close to one and a small error would produce a negative value. Instead, at the $k + 1$ iteration, P_o is defined as:

$$P_o^{k+1} = \frac{1}{1 + \dfrac{P_1^{k+1}}{P_o^k}}, \tag{11A}$$

and this is always positive. Another modification that significantly improves the convergence rate is to average $P_o(x)$ over a small interval (~ 0.5 Å) around x.

E. Iteration procedure

The numerical solution is divided into seven subroutines: POT (finds potential energy functions); PO (finds P_o at each x); H (finds integral h in Eq. 7); FLUX (finds the flux of each ion i, Eq. 7); SOLVE (solves the matrix equation for the diffuse potential, Eq. 7A); POTDIF (finds self potential, Eq. 15); POTONE (finds ϕ_1, Eq. 10A); The rate of convergence depends on the order in which these subroutines are calculated. Although the procedure has not been optimized systematically, the following order was chosen on a simple trial and error basis: H; FLUX, POT, PO, SOLVE, POT, PO, POTONE, POTDIF.

Received for publication 4 December 1989 and in final form 15 October 1990.

REFERENCES

Cooper, K., E. Jakobsson, and P. Wolynes. 1985. The theory of transport through membrane channels. *Prog. Biophys. Mol. Biol.* 46:51-96.

Dani, J. A. 1989. Site-directed mutagenesis and single-channel currents define the ionic channel of the nicotinic acetylcholine receptor. *TINS Trends Pharmacol. Sci.* 12:125-128.

deLevie, R., N. G. Seidah, and H. Moreira. 1972. Transport of ions of one kind through thin membranes. II. Non-equilibrium steady-state behavior. *J. Membr. Biol.* 10:171-192.

Imoto, K., C. Busch, B. Sakmann, M. Mishina, T. Konno, J. Nakai, H. Bujo, Y. Mori, K. Fukuda, and S. Numa. 1988. Rings of negatively charged amino acids determine the acetylcholine receptor channel conductance. *Nature (Lond.).* 335:645-648.

Levitt, D. G. 1975. General continuum analysis of transport through pores. I. Proof of Onsager's reciprocity postulate for uniform pore. *Biophys. J.* 15:533-551.

Levitt, D. G. 1985. Strong electrolyte continuum theory solution for equilibrium profiles, diffusion limitation, and conductance in charged ion channels. *Biophys. J.* 48:19-31.

Levitt, D. G. 1986. Interpretation of biological channel flux data. *Annu. Rev. Biophys. Biophys. Chem.* 15:29-57.

Levitt, D. G. 1987. Exact continuum solution for a channel that can be occupied by two ions. *Biophys. J.* 52:455-466.

Levitt, D. G. 1990. General continuum theory for multiion channel. II. Application to acetylcholine channel. *Biophys. J.* 59:278-288.